Formation and Cleavage of a DNA Network during *in Vitro* Bacteriophage T7 DNA Packaging: Light Microscopy of DNA Metabolism†

Mao Sun, Marjatta Son, and Philip Serwer*

Department of Biochemistry, The University of Texas Health Science Center, San Antonio, Texas 78284-7760

Received June 12, 1997⊗

ABSTRACT: To understand *in vivo* DNA metabolism, *in vitro* systems are developed that perform DNA metabolism, while maintaining *in vivo* (physiological) character. To determine the state of DNA during *in vitro* physiological metabolism, the present study develops procedures of fluorescence light microscopy for observation of stained DNA molecules during *in vitro* physiological metabolism in a crude extract of bacteriophage T7-infected cells. The extract inhibits illumination-induced breakage of DNA. The following DNA metabolism remains active for 2−3 min during microscopy: exonuclease-dependent end-to-end joining (concatemerization) of T7 DNA and subsequent cleavage of concatemers. When the T7 gene 3-encoded DNA debranching endonuclease is absent during *in vitro* T7 DNA concatemerization, DNA progressively partitions to form a continuous, mostly immobile (i.e., no detected Brownian motion) fibrous network that encloses the DNA-depleted solution; presumably because of reduced branching, a less extensive network forms when the gene 3-encoded debranching endonuclease is present. Most strands of the network consist of multiple DNA segments. After a time interval of 5−10 min, the DNA network undergoes cleavage that depends on the presence of both ATP, capsids, and the DNA packaging accessory proteins encoded by genes 18 and 19; multiple cleavages eventually disrupt the continuity of the DNA network. The dependence of the observed cleavage on these factors is explained by the hypothesis that this cleavage is the first of two cleavages known to occur during the packaging of T7 DNA concatemers both *in vivo* and *in vitro*. The first cleavage is also known to initiate entry of DNA into a T7 capsid. The cleavage observed here is usually preceded by an approximately 10 s burst of oscillatory motion of the DNA network near the point of eventual cleavage. If the *in vivo* presence of a similar concatemer-containing DNA network is assumed, requirement for DNA packaging-associated release of DNA from this network is a possible explanation for the evolution of a T7 DNA packaging pathway that is initiated by cleavage of a concatemer.

Analysis of DNA metabolism is currently done macroscopically, i.e., by averaging the results for numerous DNA molecules. To avoid loss of information about either the temporal order or the spatial partitioning of metabolic events, both biochemical analysis and biophysical analysis are desirable at the level of a single metabolic event. By using a fluorescent dye, single DNA molecules have been observed by fluorescence light microscopy (Matsumoto *et al*., 1981; Yanagida *et al*., 1983; Houseal *et al*., 1989; Bustamante, 1991; Minagawa *et al*., 1994; Serwer *et al*., 1995); the shape of a DNA random coil has been directly observed (Serwer *et al*., 1995). To perform light microscopy of DNA during its metabolism, a tractable biochemical system is needed.

Among the events of DNA metabolism, packaging of DNA in the preformed procapsids of bacteriophages is studied because bacteriophage DNA packaging is complex enough to be a biological process, but simple enough to be accessible to biochemical, biophysical, and genetic analysis. In the case of bacteriophage T7, extracts of T7-infected cells both join the terminally repeated 40 kilobase (kb) pair T7 DNA end-to-end (the product is called a concatemer) and package T7 concatemers in bacteriophage capsids. Concatemers are the preferred substrate for T7 DNA packaging; they are cleaved to mature length during packaging (Masker *et al*., 1978; White & Richardson, 1987a,b; Son & Serwer, 1992). *In vitro* T7 DNA packaging requires procapsids (Masker & Serwer, 1982), ATP (Masker, 1982), and two accessory proteins, p18 (White & Richardson, 1987a) and p19 (White & Richardson, 1988). Although concatemeric substrates for DNA packaging are usually assumed to exist in unpartitioned solution both *in vivo* and *in vitro*, to the authors' knowledge, no test of this assumption has been carried out. If partitioning does occur during concatemerization, this partitioning potentially will be a constraint on both the DNA packaging pathway and other DNA-metabolizing pathways that have evolved. Thus, in the present study, techniques of light microscopy have been developed for observing metabolizing DNA in T7 cell-free (*in vitro*) extracts that both concatemerize and package the DNA of bacteriophage T7; the extracts are unfractionated lysates of T7-infected cells. By using these techniques, the behavior of T7 DNA during *in vitro* concatemerization-packaging is observed. In terms of evolution, the results explain the previously made observation (White & Richardson, 1987b; Serwer *et al*., 1992) that DNA packaging is initiated by the cleavage of a concatemer to form the first DNA end packaged; a second cleavage occurs at the end of DNA packaging.

† This research was supported by both the National Institutes of Health (Grant GM24365) and the Robert A. Welch Foundation (Grant AQ-764).

* Author to whom correspondence should be addressed. Telephone: (210) 567-3765. Fax: (210) 567-6595. E-mail: Serwer@uthscsa.edu.

⊗ Abstract published in *Advance ACS Abstracts,* September 15, 1997.

S0006-2960(97)01410-4 CCC: $14.00

Table 1: Partial List of T7 Genes[a]

gene	function
gene 1	RNA polymerase
gene 2.0	inactivator of host RNA polymerase
gene 2.5	single-stranded DNA binding protein
gene 3.0	debranching endonuclease that also degrades host DNA
genes 4A and 4B	primase
gene 5	DNA polymerase
gene 6	5′→ 3′ exonuclease
gene 7	protein of the T7 capsid
gene 8	protein that connects both internal proteins and the external tail to the outer shell of a T7 capsid
gene 9	scaffolding protein (outer shell assembly)
genes 10A and 10B	major (10A) and minor (10B) proteins of the capsid's outer shell
genes 11 and 12	tail proteins
genes 13−16	proteins of an internal cylinder in the T7 procapsid
gene 17	tail fiber protein
gene 18	smaller DNA packaging accessory protein
gene 19	larger DNA packaging accessory protein

[a] Reviewed in Studier and Dunn (1983) and Steven and Trus (1986).

MATERIALS AND METHODS

Bacteriophages and Bacteriophage DNA. Both bacteriophage G and the 670 kb DNA released at 60 °C from bacteriophage G were obtained, and the DNA concentration was determined by using procedures previously described (Serwer *et al*., 1995). Bacteriophage T7 single amber mutants were received from F. W. Studier (Studier, 1969). A single amber mutant will be indicated by T7, followed by the number of the mutant gene in subscript. Double and triple amber mutants will be similarly indicated by placing all mutant genes in the subscript position. For example, T7 amber mutant in genes 3 and 5 will be called $T7_{3,5}$. The following multiple mutants were received from W. E. Masker: $T7_{3,5,6}$ and $T7_{3,5}$. The following multiple mutants were constructed by using a genetic cross: $T7_{3,18}$, $T7_{3,19}$, and $T7_{3,10}$. Additional double mutants have been previously used (Son *et al*., 1993). The permissive host for amber mutants was *Escherichia coli* 0-11′; both the nonpermissive host for amber mutants and the host for wild-type bacteriophage (indicated by a subscript wt) was *E. coli BB/1*. Both the number of a T7 gene and the function of its gene product are summarized in Table 1 for selected T7 genes (Studier & Dunn, 1983). The protein encoded by a T7 gene will be indicated by p, followed by the number of the gene. Both $T7_{wt}$ and T7 amber mutants were grown and purified by using procedures previously described (Son *et al*., 1993). Mature T7 DNA was isolated from purified bacteriophage T7 by extraction with phenol; the DNA concentration was determined from the optical density measured at 260 nm (Son *et al*., 1988). T7 DNA is 39.936 kb long (Dunn & Studier, 1983).

In Vitro Metabolism. Lysates of cells infected with T7 amber mutants were prepared by using procedures previously described (Son *et al*., 1988) with 10% dextran with a molecular weight of 10 000 present. After lysis, centrifugation was used to remove both endogenous DNA and other lysate components large enough to be imaged as background objects during fluorescence microscopy. Unless otherwise indicated, this centrifugation was performed at 2 °C, in a Beckman TL-100 tabletop ultracentrifuge; two successive centrifugations were performed for 5 min at 60 000 rpm. When indicated, the single centrifugation previously used in Son *et al*. (1988) (also 5 min at 60 000 rpm and 2 °C) was also used here. A lysate will be named by the bacteriophage used to infect the cells that were used to make the lysate. In some cases, two lysates will be mixed (equal volumes). This mixture will be named by the bacteriophages that were used to make its component lysates. For example, the mixture of a $T7_{4,9}$ lysate and a $T7_{5,19}$ lysate will be called a $T7_{4,9} + T7_{5,19}$ lysate. The final mixture will also be called a DNA-metabolizing extract. To add p6 (a 5′ → 3′ exonuclease; Kerr & Sadowski, 1972) to an extract missing p6, purified p6 (obtained from United States Biochemicals, Cleveland, OH) was added to an extract (1 part of p6 per 10 parts of extract) before addition of DNA.

To initiate DNA metabolism, a DNA-metabolizing extract (30 parts) was added to mature T7 DNA (1 part); the extract−DNA mixture was incubated at the temperature indicated. To examine a DNA−extract mixture by light microscopy at several times after the beginning of incubation, the DNA−extract mixture was initially divided into separate culture tubes; at several times, DNA was taken from an unused culture tube and prepared for fluorescence microscopy by using procedures described in the next section. Micrographs were obtained only during the first 2 min of observation. The total time of incubation is shown in the figures. The dextran present in DNA-metabolizing extracts caused an increased background-associated slight loss of resolution of stained DNA during fluorescence microscopy.

Fluorescence Light Microscopy. To perform fluorescence light microscopy, a mixture of DNA and DNA-metabolizing extract (29 μL) was added to a solution of fluorescent dye (1 μL). Unless otherwise indicated, the dye was 4′,6-diamidino-2-phenylindole (DAPI)[1] (Matsumoto *et al*., 1981; Bustamante, 1991). This mixture was placed on a flat microscope slide that was subsequently both covered by a flat cover glass and placed on a temperature-regulated (Peltier cell) copper stage on an Olympus BH2 fluorescence microscope used with both ultraviolet illumination and an orange emission filter. When DNA was stained with ethidium, fluorescence microscopy was performed by using procedures previously described (Serwer *et al*., 1995). The copper stage was both designed and constructed by N. L. Criscimagna. The time of specimen preparation was less than 0.5 min; to minimize this time, silicone grease (instead of nail polish) was used to seal the edge of the cover glass. When indicated, T7 DNA was stretched during light microscopy by exerting pressure on the cover glass (Serwer *et al*., 1995). Procedures for both recording images via image intensifier-videotape and reproducing these images are those previously described (Serwer *et al*., 1995). To quantify fluorescence, videotaped images were obtained without the image intensifier; intensity (background subtracted) per micrometer of fiber length (I_L) was measured in arbitrary units from an image digitized by using procedures previously described (Serwer *et al*., 1995). To correct for nonlinearity in the response of the recording system, an optical step wedge, illuminated through an orange filter, was imaged directly by the video camera.

[1] Abbreviations: DAPI, 4′,6-diamidino-2-phenylindole; I_L, fluorescence intensity per length of a fiber; PFGE, pulsed field agarose gel electrophoresis; *n*, number of DNA double helixes across the diameter of a DNA fiber; Nc, number of cleavage events per minute per square micrometer; *t*, time; *F*, frequency of values of I_L.

Expression of Cloned Proteins. To express a single T7 protein that was to be added to a DNA-metabolizing extract, one of the following pET-1-based expression vectors in *E. coli* HMS174 cells (Studier *et al*., 1990) was induced at 2 $\times$ 10^8 cells/mL, by addition of isopropyl β-thiogalactoside (9.5 μg/mL); the cells had been grown at 30 °C in the presence of ampicillin (200 μg/mL): pAR2652 (p18), and pAR2326 (p19). Both gene 18 and gene 19 were cloned behind the T7 Ø10 promoter (Rosenberg *et al*., 1987); both vector-containing strains were received from A. Rosenberg. To obtain a control that had not expressed any T7 protein, the parent strain (i.e., a strain that was the same, except for the absence of a cloned gene) was induced. After induction, growth was continued for 60 min at 37 °C. The induced cells were both pelleted and lysed by using the procedure used to prepare a DNA-metabolizing extract.

Pulsed Field Agarose Gel Electrophoresis. To determine the length of T7 DNA after it had been incubated in a DNA-metabolizing extract, the DNA−extract mixture (10 μL) was RNase-digested, protease-digested, and then heated to 75 °C (raising temperature expelled packaged DNA) by using the procedures in Son *et al*. (1988). Subsequently, the extract was subjected to pulsed field agarose gel electrophoresis (PFGE) through a 1.2% agarose gel (Seakem LE agarose; FMC Bioproducts, Rockland, ME) cast in 0.09 M Tris-acetate (pH 8.4) and 0.001 M EDTA. Pulsing of the electrical field was achieved with microprocessor-controlled periodic rotation of the gel from orientation angle -0.3π to orientation angle 0.3π and back; the procedures of Serwer *et al*. (1995) were used. During PFGE, the time at each of these two orientations (pulse time) was 40 s; the temperature was 20 $\pm$ 0.2 °C, and the electrical field was 2 V/cm. After PFGE, the gel was stained with 1 μg/mL ethidium bromide for 2 h in electrophoresis buffer; the gel was subsequently destained and photographed (Son *et al*., 1988).

RESULTS

Observation of DNA in T7 DNA-Metabolizing Extracts. Among the potential limitations of performing fluorescence light microscopy of stained DNA in DNA-metabolizing extracts, the following were initially anticipated. (1) Non-DNA components of the extract reduce the clarity of images of the DNA. (2) The illumination of the microscope causes the DNA to break. (3) Metabolism in the extract is inhibited by either the stain or the illumination (or both). When attempts were made to stain extract-contained DNA with ethidium, images of the DNA (not shown) were considerably less clear than they were in a previous study (Serwer *et al*., 1995) performed without the extract. In contrast, when staining was performed with DAPI, comparatively sharp images of extract-contained DNA were obtained. Unlike the results obtained in the absence of an extract (Bustamanate, 1991; Serwer *et al*., 1995), no breakage of DAPI-stained DNA was observed when either single DNA molecules or the DNA networks described below were continuously observed in $T7_{3,5,6}$ extracts for times as great as 5 min (data not shown). That is, the extract inhibited the light-DAPI-induced breakage of DNA. Thus, the first two potential limitations were overcome by using DAPI to stain the DNA present in a T7 DNA-metabolizing extract. Although DAPI-stained DNA undergoes photobleaching in the absence of a DNA-metabolizing extract (Bustamanate, 1991), after 2 min of exposure to the illumination of the microscope, DAPI-stained DNA in a T7 DNA-metabolizing extract did not detectably experience photobleaching.

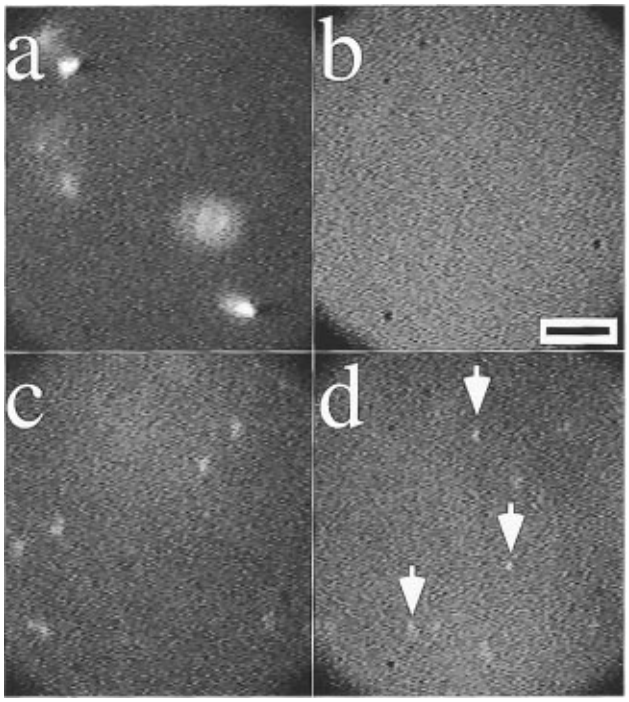

FIGURE 1: Light microscopy of DNA in an extract missing p3, p5, and p6. The following were added to a $T7_{3,5,6}$ extract prepared either (a) with the procedure of Son *et al*. (1988) or (b−d) with the procedure in Materials and Methods that includes more extensive centrifugation for clarifying the extract: (a) nothing added, (b) nothing added, (c) bacteriophage G DNA (0.5 μg/mL), and (d) bacteriophage T7 DNA (0.1 μg/mL). The magnification bar is 50 μm long. Note that images in Figure 1 are less magnified than images in subsequent figures.

To determine whether *in vitro* T7 DNA packaging was inhibited by DAPI (third potential limitation, above), *in vitro* packaging was assayed in the presence of DAPI, by quantifying the formation of infective T7 particles in the $T7_{4,9}$ + $T7_{5,19}$ extract previously used (Son *et al*., 1993). The result was that no more than 20% inhibition was caused by DAPI at concentrations either equal to or less than 0.5 μg/mL. As the concentration of DAPI increased above 0.5 μg/mL, formation of infective particles was progressively inhibited, until complete (>99.9%) inhibition occurred at 8 μg/mL. These results are similar to those obtained for bacteriophage T3 (Fujisawa *et al*., 1987). Fortunately, 0.5−1.0 μg/mL is the range of DAPI concentrations found by inspection to be optimal for visualization of DNA in T7 DNA-metabolizing extracts (data not shown).

When a $T7_{3,5,6}$ DNA-metabolizing extract was prepared by using procedures previously described (Son *et al*., 1993), without addition of exogenous DNA, observation by light microscopy (the stain was 0.5 μg/mL DAPI) revealed sufficient endogenous DNA (from either the host or the infecting bacteriophage or both) to interfere with visualization of exogenous DNA. A typical field of this $T7_{3,5,6}$ extract is shown in Figure 1a. Without a loss in an extract's capacity for producing infectious T7, visible endogenous DNA was almost completely eliminated by the more extensive of the two procedures of centrifugation described in Materials and Methods (Figure 1b). However, some endogenous DNA did appear to be present, but adhered to the microscope slide; the adhered DNA was not imaged, but did create background

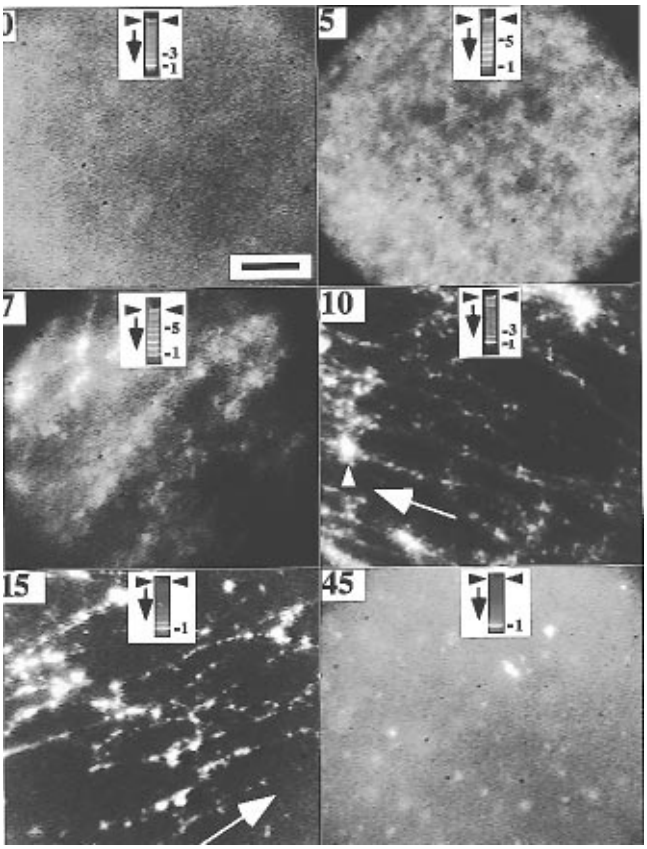

FIGURE 2: Images as a function of time in an extract missing only p3 and p5. To a $T7_{3,5,6}$ extract that contained p6 (1.5 units/mL) was added T7 DNA (100 μg/mL); this mixture was incubated at 30 °C. Images obtained by fluorescence microscopy were formed at the time (minutes) indicated at the upper left of each panel. A portion of an extract was prepared for PFGE; after PFGE for 48 h, the pattern obtained is in the middle of the corresponding panels. In the PFGE profiles, the numbers indicate the length of a DNA in units of one mature T7 DNA length; the arrows indicate the direction of electrophoresis; the arrowheads indicate the origins of electrophoresis. The white arrowhead indicates a nodule; the white arrow indicates the direction of preferential orientation of fibers. For the light micrographs, the magnification bar is 10 μm long.

fluorescence. This DNA may have been attached to a glass-adherent cell membrane or wall component of *E. coli*. When bacteriophage G DNA (0.5 μg/mL) was added to a $T7_{3,5,6}$ extract, the mobile (i.e., undergoing Brownian motion) asymmetrical random coils previously observed in buffer (Serwer *et al*., 1995) were again observed, though not as clearly (Figure 1c). When T7 DNA (0.1 μg/mL) was added to a $T7_{3,5,6}$ extract, smaller, more mobile DNA molecules were observed (indicated by arrows in Figure 1d). Thus, the more extensive centrifugation used to clarify the extract of Figure 1b will also be used to clarify extracts in the experiments described below.

The $T7_{3,5,6}$ extract used above is missing the three T7 DNA-metabolizing gene products whose effects should be the most easily detectable by microscopy of DNA (Table 1). When either T7 or G DNA was added to a $T7_{3,5,6}$ extract and incubated for a time as long as 2 h, no effect of the extract on the DNA was observed by light microscopy (data not shown). Thus, interaction of T7 DNA with extract components other than p3, p5, and p6 did not have a visible effect on the DNA.

Effects of Gene 6 Exonuclease (p6): Formation of a DNA Network. To determine the effect of concatemerization on DNA in an *in vitro* T7 DNA-metabolizing extract, p6 (1.5 units/mL, final concentration) was added to a $T7_{3,5,6}$ extract. The p6 is known to stimulate concatemerization of monomeric T7 DNA; the mechanism of stimulation is generation of complementary single-stranded T7 DNA ends by exonucleolytic digestion of the terminally repeated T7 DNA (Son & Serwer, 1992). Immediately after addition to the p6-containing $T7_{3,5,6}$ extract of T7 DNA at a concentration of 100 μg/mL (the concentration previously used for *in vitro* T7 concatemerization-packaging; Son *et al*., 1988, 1993; Son & Serwer, 1992), fluorescence microscopy of the DNA-containing extract revealed no visible features. Single DNA molecules were not discerned because the DNA concentration was so high that overlapping among DNA molecules eliminated the contrast between the background solution and the DNA. This result is shown in Figure 2a for the $T7_{3,5,6}$ extract to which p6 had been added; the time after addition of T7 DNA (minutes) is indicated in the upper left of each panel. However, as time increased to 5−10 min during incubation of a p6-containing extract at 30 °C, light microscopy revealed a progressive partitioning of DNA to form a network that consisted of a predominantly fibrous DNA-rich phase that, in projection, surrounded zones of a comparatively DNA-poor phase (Figure 2). All images in Figure 2 were obtained less than 0.5 min after preparation of a portion of the DNA−extract mixture for light microscopy. When a preparation was illuminated on the fluorescence microscope stage for a time greater than 1−2 min, the changes in Figure 2 stopped; images remained static for times as great as 2 h. Control experiments (not shown) revealed that the stopping of metabolism was caused primarily by the illuminating beam of the microscope; in the absence of the illuminating beam, metabolism was progressively lost in a period of 1−2 h.

To determine whether, as expected, the DNA network contained concatemers, analysis by PFGE was performed on samples taken from the extract used for Figure 2. The result was the progressive formation of concatemers as time increased to 7−10 min (for a panel in Figure 2, the PFGE profile is displayed at the upper middle part of the panel; the numbers next to the PFGE profile indicate the number of 40 kb pair T7 genomes in a band-forming concatemer). Subsequently, monomeric T7 DNA progressively dominated the PFGE profile. Thus, the network is assumed to contain concatemers. The network apparently dissolved either during dilution for PFGE or during entry of DNA into the gel used for PFGE.

Along fibers observed at 10 and 15 min in Figure 2, both the width and the intensity varied. Most fibers were decorated by wider DNA condensates (to be called nodules; one of the larger nodules is indicated by an arrowhead in the 10 min panel of Figure 2). As partitioning occurred, sometimes partial orientation of the fibers also occurred. For example, in the 10 and 15 min panels of Figure 2, the DNA fibers are preferentially oriented in the direction indicated by the arrows. Along more than 90−95% of the length of DNA fibers in the networks present between 10 and 15 min in Figure 2, the main fibers seen in Figure 2 exhibited no detectable Brownian motion. However, in the intranetwork spaces, some DNA segments, possibly loosely attached to the DNA network, did undergo Brownian motion.

Cleavage of the DNA Network. As time progressed above 7−10 min in Figure 2, the DNA network experienced visible

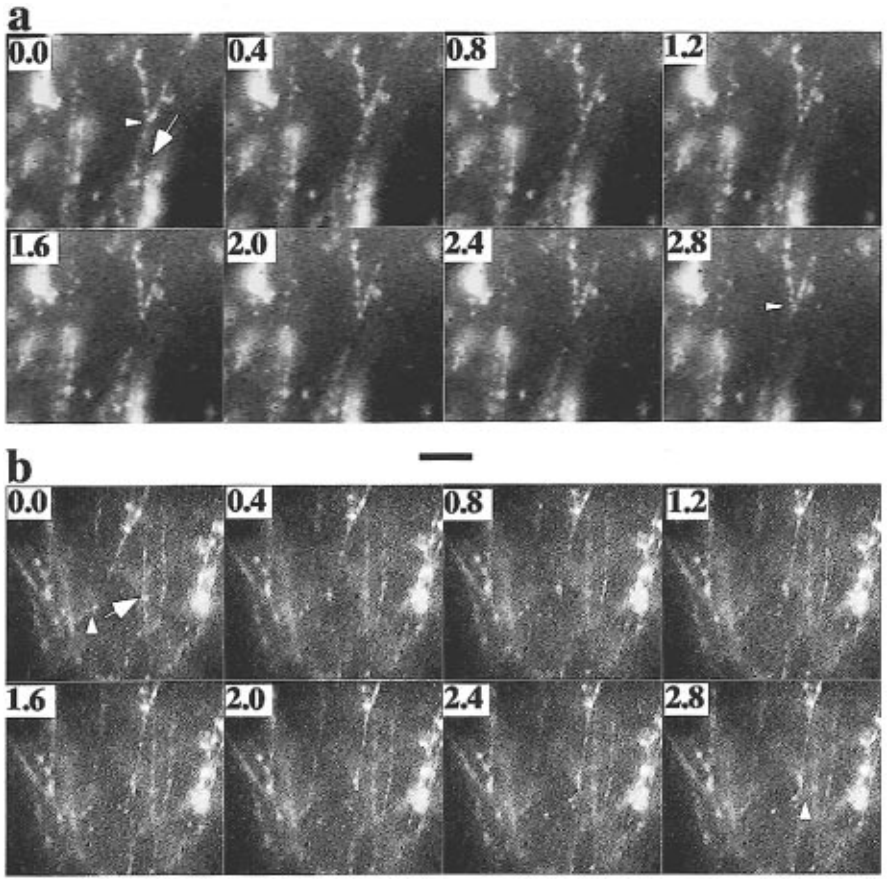

FIGURE 3: Cleavage of a DNA network. A p6-supplemented (1.5 units/mL) $T7_{3,5,6}$ DNA-metabolizing extract−T7 DNA mixture (100 μg of DNA/mL) was incubated at 30 °C. (a and b) Images of the DNA network near two points of cleavage are shown. A point of cleavage is indicated by an arrowhead; the direction of postcleavage motion is indicated by an arrow. The time (seconds) of an image is indicated in the upper left of a panel. The zero times of the figure both correspond to approximately 20 min after the start of incubation. Note the difference between the time scale in Figure 3 (seconds) and the time scale in Figure 2 (minutes). The bar is 10 μm long.

effects of cleavages. The earliest cleavages were revealed by the movement of one part of the network away from the adjacent part of the network. After an initial, sudden movement, separation usually continued for 2−15 s. In Figure 3a,b, examples are shown for two independent videotaped sequences; the time (seconds) of each frame is given at the upper left; an arrowhead indicates the approximate point of cleavage before separation in the direction of the arrow. Possibly, additional cleavages occurred that did not have visible effects. The number of cleavages was large enough so that, as time progressively increased to 45 min in Figure 2, the network lost its continuity. As shown in the PFGE profiles of Figure 2, monomeric DNA is the primary cleavage product. The region of the PFGE profiles below the region shown in Figure 2 did not have sufficient DNA to detect by ethidium staining; the gel would have revealed a linear DNA as small as 5 kb.

Although cleavage was apparent from 15 to 30 min in the experiment of Figure 2, qualitiatively, cleavage was not obvious at 10 min, even though the DNA network was present; quantification of this effect is described in a subsequent section. The quiescent period for cleavage is explained with the assumption that cleavage is caused by a metabolic event that requires an initiation time of several minutes. Possibly, this event is DNA packaging. Further tests of this possibility are also described in a subsequent section.

Amount of DNA per Fiber in the DNA Network. Because of the limits to the resolution of light microscopy (0.5−1.0 μm; Slayter & Slayter, 1992), the number of double-stranded DNA segments (n) across the diameter of each observed DNA fiber (Figures 2 and 3) cannot be determined by separately resolving these double-stranded DNA segments. Instead, n was determined by quantifying I_L for both a network-associated fiber and a fiber for which n was reasonably assumed to be 1. For fibers observed in a p6-supplemented $T7_{3,5,6}$ extract at 15 min after the start of incubation, the distribution was determined for I_L; fibers were selected at random; nodules were not included. The result was that the highest I_L values were 4−5 times greater than the lowest I_L values; a frequency (F) vs I_L plot (Figure 4) had two peaks. If (1) I_L is assumed to be proportional to the number of double-stranded DNA segments per observed fiber and (2) the lowest I_L value is assumed to be the I_L value of a single DNA double helix, then the peaks in the F vs I_L plot are at approximately 2 and 3 DNA double helixes per observed fiber. The brightest fibers have 4−5 DNA double helixes per fiber, but the F values for these fibers were not high enough to form a peak in Figure 4. To independently determine I_L for a double-stranded DNA segment, the I_L for unconcatemerized T7 DNA that had been stretched was determined (Materials and Methods) during light microscopy of T7 DNA at 0.1 μg of DNA/mL. When compared to the lowest I_L of a fiber within a network formed by a p6-supplemented $T7_{3,5,6}$ extract, the I_L of a stretched T7 DNA was 0.96 ± 0.06 times as great. Microscopy for this comparison was performed without changing any aspect of the system for either obtaining or recording images. Thus,

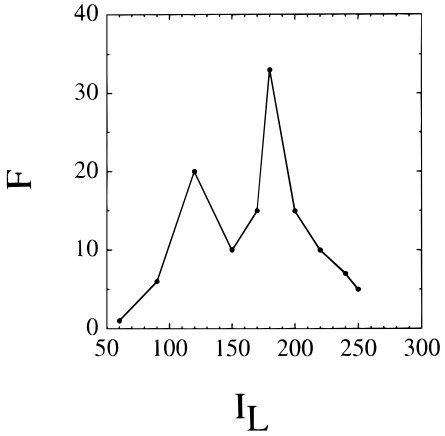

FIGURE 4: Number (n) of DNA segments across the diameter of network-forming DNA fibers. To determine n, values of I_L were determined for randomly selected, network-forming DNA fibers within a $T7_{3,19}$ DNA-metabolizing extract−T7 DNA mixture (100 μg of DNA/mL) that had been incubated at 30 °C for 15 min. The frequency (F) of I_L values is plotted as a function of I_L.

the I_L for $n = 1$ was confirmed, as was the conclusion that peak n values were 2−3. However, the arrangement of the multiple double-helical DNA segments within a network-associated fiber cannot be deduced from the current data. The fiber cleaved in Figure 3a appears to consist of more than one DNA double helix; the fiber cleaved in Figure 3b appears to consist of a single DNA double helix.

Effects of p3-Debranching Endonuclease. The extracts used for Figures 1−4 were all missing p3, a DNA-debranching endonuclease known to be necessary for at least one recombination pathway of T7 DNA both *in vivo* (Ogawa *et al*., 1978; Panayotatos & Fontaine, 1987) and *in vitro* (Lee & Sadowski, 1983; De Massy *et al*., 1987; Parsons & West, 1990). To help determine the effects of p3, the DNA in a $T7_3$ extract (i.e., an extract missing only p3) was compared to the DNA in a $T7_{4,9} + T7_{5,19}$ extract (i.e., an extract not missing any T7 protein). In the $T7_3$ extract, the network formed, as it had in the p6-supplemented $T7_{3,5,6}$ extract; between 5 and 60 min, fluorescence microscopy revealed no significant difference between these two extracts (data not shown). In the $T7_{4,9} + T7_{5,19}$ extract, the network formed [Figure 5; time (minutes) is indicated at the upper left of each panel] but was never as extensive as the network formed in the absence of p3. As also found for the network in the p6-supplemented $T7_{3,5,6}$ extract in Figure 2, the network in the $T7_{4,9} + T7_{5,19}$ extract fragmented as time progressed beyond 15 min in Figure 5.

The enhancement of network formation by the removal of p3 indicates that increasing the concentration of branched DNA molecules promotes assembly of the DNA network. Branched molecules presumably are among those at the origin in the PFGE profiles in Figures 2 and 5. Analogously, formation of the network of comparatively thick fibers of an agarose gel is promoted by branching of constituent thinner agarose fibers (Dea *et al*., 1972). Thus, a p3-induced decrease in network formation is expected.

Source of the p3-Independent Cleavage of the DNA Network. One possible source of the p3-independent cleavage of the DNA networks of Figures 2 and 3 is the p18- and p19-dependent cleavage that initiates T7 DNA packaging (White & Richardson, 1987a,b, 1988; Fujisawa *et al*., 1990). To help determine whether the cleavage observed by light

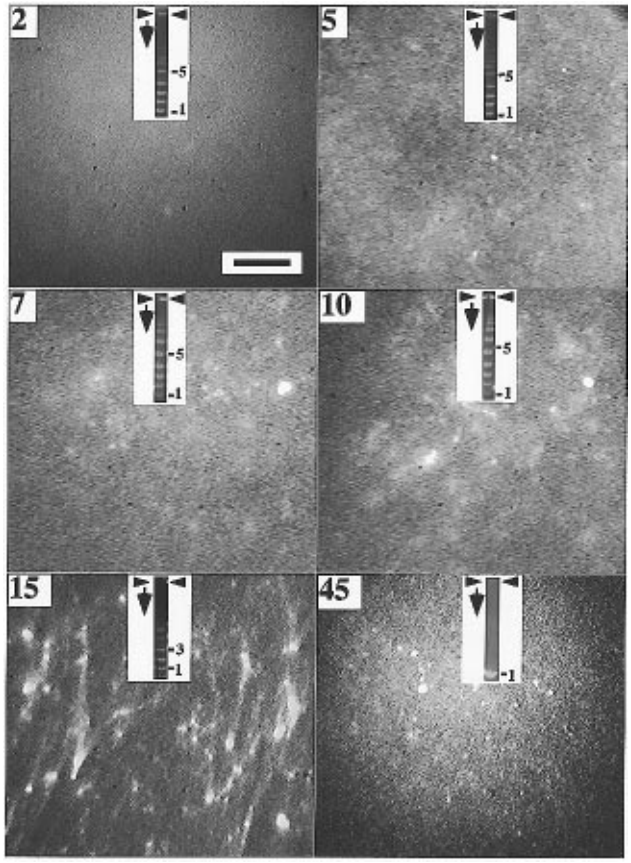

FIGURE 5: Images as a function of time in an extract not missing any T7 proteins. To a $T7_{4,9} + T7_{5,19}$ extract was added T7 DNA (100 μg/mL); this mixture was incubated at 30 °C. Images obtained by fluorescence microscopy were obtained at the time (minutes) indicated at the upper left of each panel. A portion of an extract was diluted for PFGE; after PFGE for 63 h, the pattern obtained is in the middle of the corresponding panels. In the PFGE profiles, the numbers indicate the length of a DNA in units of one mature DNA length; the arrows indicate the direction of electrophoresis; the arrowheads indicate the origins of electrophoresis. The magnification bar is 10 μm long.

microscopy initiates *in vitro* T7 DNA packaging, the extent of cleavage in the absence of p19 was compared to the extent of cleavage in the same extract to which p19 had been added. To quantify the extent of cleavage, the number of cleavage events per minute per square micrometer (Nc) was determined by using fields that were illuminated for no more than 60 s. When Nc was plotted as a function of time (t), a $T7_3$ extract yielded a Nc(t) plot that had a peak 30 min after the start of incubation, i.e., 20−25 min after the DNA network first formed ($T7_3$ plot in Figure 6a). In contrast, a $T7_{3,19}$ extract yielded a flat Nc(t) plot for which Nc was always 10-fold less than the peak Nc of the $T7_3$ extract ($T7_{3,19}$ plot in Figure 6a; in both the $T7_3$ and the $T7_{3,19}$ extracts, the network was indistinguishable from the network in Figure 2). This difference was dramatic enough to be easily perceived by visual inspection of the original videotapes. To determine whether p19 could restore the cleavage activity of the $T7_{3,19}$ extract, the $T7_{3,19}$ extract of Figure 6a was supplemented with p19 from a lysate of the induced p19 expression vector. The result was restoration of cleavage ($T7_{3,19}$ + p19 in Figure 6a); no significant effect was observed when a control lysate without p19 was used (not shown). To determine the effect of changing the concentration of p19, the Nc observed at 30 min was determined as a

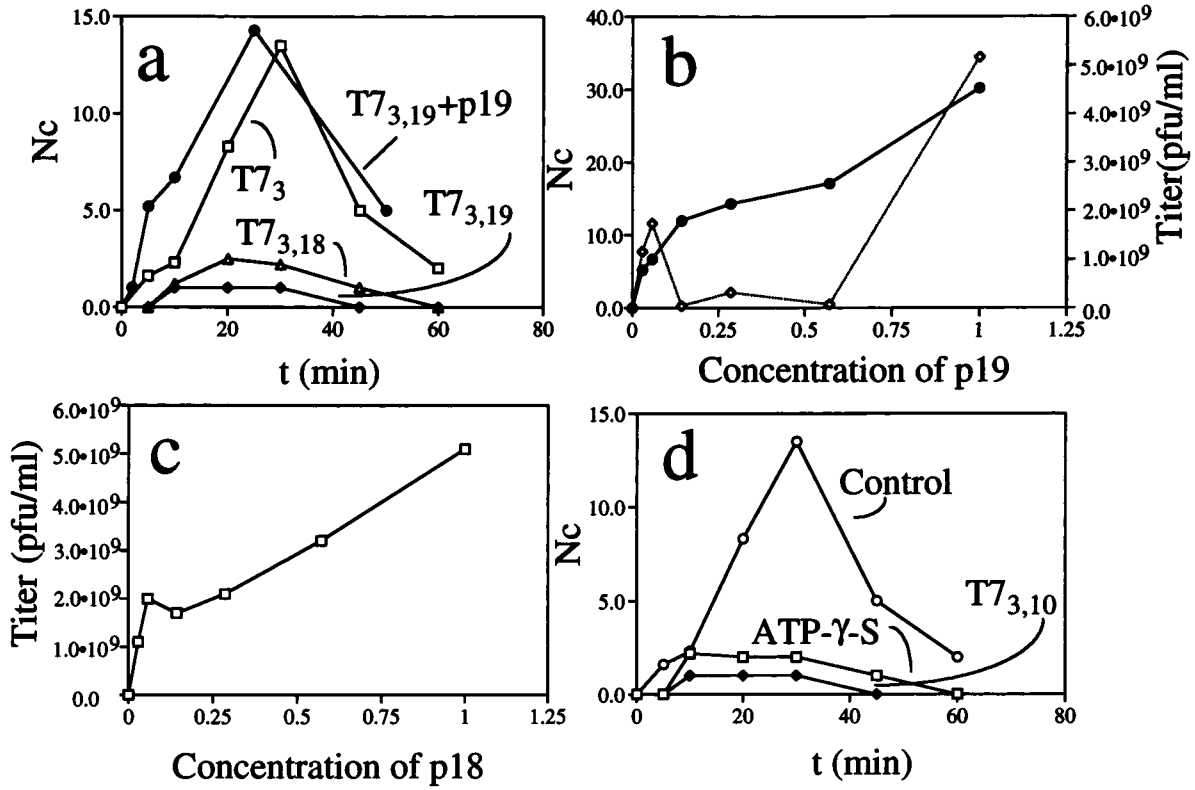

FIGURE 6: Quantitative analysis of the cleavage of the DNA network. (a) A plot of Nc vs *t* is made for the following extracts indicated in the figure: $T7_3$, an unsupplemented $T7_3$ extract; $T7_{3,19}$, an unsupplemented $T7_{3,19}$ extract; $T7_{3,19}$ + p19, a $T7_{3,19}$ extract that had been supplemented with an extract of the induced p19 expression vector (the latter was diluted by a factor of 5); and $T7_{3,18}$, an unsupplemented $T7_{3,18}$ extract. (b) (Solid line and left vertical axis) A plot of Nc is made at $t = 30$ min as a function of the concentration in a $T7_{3,19}$ extract of a p19 supplement obtained by inducing the p19 expression vector. The concentration of the undiluted supplement is 1.0. (Dashed line and right vertical axis) The same plot is made for the yield of infective particles per milliliter of extract, after incubating for 60 min at 30 °C. (c) A plot is made at $t = 30$ min for the yield of infective particles, as a function of the concentration in a $T7_{3,18}$ extract of a p18 supplement obtained by inducing the p18 expression vector. The concentration of the undiluted supplement is 1.0. (d) A plot of Nc vs *t* is made for either a $T7_{3,10}$ extract (labeled $T7_{3,10}$) or a $T7_{4,9}$ + $T7_{5,19}$ extract, the latter of which was mixed with either ATP-γ-S (25 mM final concentration; labeled ATP-γ-S) or water (labeled control) by 1:10 dilution. Presumably because of increased DNA branching, both the $T7_3$ and the p19-supplemented $T7_{3,19}$ extracts had yields of infectivity that were lower than those previously described (Son *et al*., 1988) for extracts not missing p3.

function of the concentration of p19 added via a lysate of the induced p19 expression vector. The result was cleavage that increased as the amount of added p19 increased (solid line in Figure 6b). Thus, most (>98%) cleavages of the DNA network occurred if and only if p19 was present.

To determine whether the p19-dependent cleavages yielded infectious bacteriophage particles, the p19−extract mixtures of Figure 6b were incubated until production of infectious particles normally stopped (60 min); the titer of infective particles was determined (dashed line in Figure 6b). Addition of p19 did increase the yield of infective particles. As the concentration of p19 increased, two peaks were observed in the yield of infective particles per milliliter. The observation of these two peaks was reproducible (three independent experiments). The data of Figure 6b support the conclusion that the p19-dependent cleavage yields a substrate for DNA packaging. Because the p19 of the T7-related bacteriophage, T3, is a DNase (Fujisawa *et al*., 1990), p19 is probably the enzyme that cleaves the DNA network in Figure 3. The complexity of the response of infective particle production to p19 concentration is not understood.

Although p18 is not known to have either a nuclease activity or a role in capsid I assembly, p18 is, like p19, required for T7 DNA packaging (White & Richardson, 1987b,c). Thus, the effect on cleavage of removing p18 was determined by performing light microscopy of T7 DNA in a $T7_{3,18}$ extract. Like the $T7_{3,19}$ extract, a $T7_{3,18}$ extract yielded a DNA network when incubated with T7 DNA (not shown). The $T7_{3,18}$ network experienced the same low-level cleavage that the $T7_{3,19}$ extract experienced (Figure 6a). To determine whether p18 could restore the cleavage activity of the $T7_{3,18}$ extract, the experiment of Figure 6b was repeated by using a $T7_{3,18}$ extract and a p18 expression vector. For infective particle production, the result (shown in Figure 6c) was similar to that obtained for the $T7_{3,19}$ extract and p19 expression vector in Figure 6b; the valley between peaks was, however, not as deep in Figure 6c. For cleavage of the network, the effect of p18 was to completely eliminate the network, even at the lowest concentration of Figure 6c. Thus, the cleavage that required a known nuclease, p19, also required the accessory protein, p18, known (White & Richardson, 1987a,b) to also be required for DNA packaging-associated cleavage of T7 concatemers. The comparatively great effect of p18 on cleavage is not understood.

In addition to p18 and p19, both ATP and a T7 procapsid are known to be necessary for T7 DNA packaging (Roeder & Sadowski, 1977; Masker, 1982; Masker & Serwer, 1982; White & Richardson, 1987b; Serwer *et al*., 1990). To determine whether ATP is also required for the DNA cleavage observed by light microscopy, cleavage in a $T7_{4,9}$ + $T7_{5,19}$ extract was quantified during incubation with T7 DNA both in the presence of 25 mM ATP-γ-S (ATP-γ-S in

Figure 6d) and in the absence of ATP-γ-S (control in Figure 6d). The ATP-γ-S inhibited cleavage of DNA. Thus, the observed cleavage of DNA requires cleavage of ATP. To determine whether capsids were required for the DNA cleavage observed by light microscopy, cleavage in a $T7_{3,10}$ extract was quantified during incubation with T7 DNA; gene 10 encodes the major protein of both the T7 procapsid and the mature T7 capsid (Table 1). The result was no cleavage above background (Figure 6d; $T7_{3,10}$). The $T7_{3,10}$ extract used produced infective bacteriophage particles when mixed with a $T7_{3,19}$ extract (2.9×10^{10} infective units/mL). Thus, the $T7_{3,10}$ extract was active. Therefore, the conclusion is drawn that, in addition to ATP, p18, and p19, the T7 procapsid is also required for the DNA cleavage observed by light microscopy.

Motion of the DNA Network before Cleavage. The data presented above are explained by the assumption that the cleavage observed is caused by the process of DNA packaging; possibly, this cleavage is the cleavage previously found to initiate DNA packaging (White & Richardson, 1987b; Serwer *et al*., 1992). If so, then both specific DNA−capsid binding and, possibly, a search by capsid I for its binding site(s) should occur before cleavage. Although DNA network-associated capsids cannot yet be detected by fluorescence light microscopy, capsid-induced DNA motion can be detected. To determine whether motion of the DNA network occurred before cleavage events, the behavior of the DNA network was determined in the time interval immediately before a visible cleavage event. Of 100 cleavage events, 67 were preceded by apparently random motion of the DNA network; this motion was visually detected without difficulty. The motion lasted roughly 10 s. When 58 similar locations were randomly selected in the DNA network, only 5 of them exhibited any detectable motion in the 10 s time interval preceding cleavage. Thus, the random motion is significantly correlated with post-motion cleavage of the DNA network.

DISCUSSION

In this study, two questions have been asked that are fundamental to both DNA packaging and other aspects of DNA metabolism. (1) During metabolism, are DNA molecules in homogeneous solution? Alternatively, are the DNA molecules selectively partitioned? (2) If partitioning occurs, what constraints does partitioning introduce for the pathways of DNA metabolism? What aspects of metabolic pathways are explained by these constraints (if any)? Thus far, answering these questions has not been possible with analysis of *in vivo* DNA metabolism. In this study, attempts have been made to answer these questions by analyzing *in vitro* DNA metabolism in a system that has the components of the *in vivo* system, though at lower concentration. At *in vivo* concentration, the nonspecific effects of cytoplasmic macromolecules, including possibly both decreasing of water activity and increasing of excluded volume [reviewed in Parsegian *et al*. (1986), Minton (1990), and Zimmerman and Minton (1993)], have been at least partially mimicked by including a neutral polymer (dextran) in the T7 DNA-metabolizing extract. The answer to the first question is that, when concatemerization is induced by the presence of p6, partitioning to form a gel-like network does occur. This partitioning is increased by removing p3 from the extract, an observation that is interpreted by the assumption that DNA branching promotes, and is possibly necessary for, formation of the network. Although concatemerization has thus far occurred in all conditions for which network formation occurred, the data do not reveal whether concatemerization is absolutely necessary for the formation of a DNA network. As found *in vitro*, during either a $T7_{wt}$ or a $T7_3$ infection, both concatemerization and branching also occur *in vivo*; branching is increased in the $T7_3$ infection (Serwer *et al*., 1990). Thus, the assumption is made that a smaller version of the network observed here also forms during *in vivo* T7 DNA metabolism.

If network-associated DNA is to be packaged, then the immobility of the network implies the constraint that DNA must be freed (possibly by cleavage) from the network before it can enter into a bacteriophage capsid. If the DNA network forms *in vivo*, this conclusion is consistent with the previous demonstration that the T7 (and T3) DNA packaging pathway is initiated by cleavage of a concatemer to form a mature right end that is subsequently the substrate for DNA packaging both *in vitro* (White & Richardson, 1987b) and *in vivo* (Serwer *et al*., 1992). The data presented here indicate that the observed cleavage is ATP-, capsid-, p19-, and p18-dependent. This cleavage is associated with an increase in the yield of infectious particles. The production of infectious particles supports the conclusion that packageable DNA is freed from the network by cleavage. The observed dependence on ATP, capsids, p19, and p18 indicates that this cleavage is not the nonspecific, DNA packaging-independent cleavage previously demonstrated (Fujisawa *et al*., 1990) in nonphysiological conditions (low ATP), for the p19 of bacteriophage T3. That is, the cleavage observed by light microscopy is part of (presumably initiates) the process of DNA packaging. If so, then the ATP-γ-S inhibition of DNA cleavage (Figure 6d) confirms that ATP cleavage is required for the initiation of T7 DNA packaging. In summary, the following hypothesis explains the evolution of a DNA packaging pathway initiated by cleavage: Before DNA can be packaged, the DNA must be released (cleaved) from an intracellular DNA network similar to the network observed *in vitro*. In analogy to the conclusion for T7, cleavage of a concatemer also appears to initiate packaging of the DNA concatemers of bacteriophages λ [reviewed in Catalano *et al*. (1995)] and P22 [reviewed in Casjens (1989)].

Although T7 concatemers are the preferred substrate for physiological T7 DNA packaging, T7 monomers and even nonhomologous DNA are also packaged (Son & Serwer, 1992). The preferential packaging of concatemers was explained by the assumption (Son *et al*., 1993) that, during initiation of T7 DNA packaging, capsid I bound a concatemer at two identical nucleotide sequences, one on each of two successive genomes within a concatemer; this nucleotide sequence is presumably part of a right end-proximal sequence shown (Chung & Hinkle, 1990) to be necessary for the packaging of plasmids by T7 capsids. However, if concatemers are part of a DNA network, forming the proposed DNA−capsid I complex will involve rearranging the network. A possible (though not demonstrated) explanation of the precleavage motion observed here is the sliding of at least one DNA segment along a capsid I particle. By this hypothesis, the sliding is part of a (possibly ATP-driven) search by the capsid for either one or both of the two DNA binding sites. To test this explanation, procedures must be developed for observing capsids by fluorescence microscopy

during *in vitro* DNA metabolism.

The observations made here appear to be the first observations by light microscopy of a single event of complex DNA metabolism. Despite the chemical complexity of the *in vitro* system, in the present study, both single and partitioned DNA molecules were observed. The observation of DNA cleavage was assisted by the presence of the DNA network. Without this network, the effects of cleavage would not have been as dramatic as those observed in Figure 3. Beyond the limited resolution of light microscopy, the primary limitations of the techniques used here were (1) the microscopy-associated loss of activity of the *in vitro* DNA-metabolizing extracts and (2) the obscuring of single double-helical DNA segments by partitioning to form the thicker fibers of the observed DNA network. However, as illustrated by the studies presented here, these limitations do not, in general, prevent the gathering of information about DNA metabolism at the level of a single event.

ACKNOWLEDGMENT

We thank Dr. Donna Louie for performing preliminary experiments that demonstrated the feasibility of the studies described here, Dr. Alan Rosenberg for providing expression vectors, Dr. Gary A. Griess for advice in performing image processing, Karen Lieman and Michele Gates for technical assistance, and Linda C. Winchester for typing the manuscript.

REFERENCES

Bustamante, C. (1991) *Annu. Rev. Biophys. Biophys. Chem. 20*, 415−446.
Casjens, S. (1989) in *Chromosomes: Eukaryotic, Prokaryotic and Viral* (Adolph, K. W., Ed.) Vol. 3, pp 241−261, CRC Press, Boca Raton, FL.
Catalano, C. E., Cue, D., & Feiss, M. (1995) *Mol. Microbiol. 16*, 1075−1086.
Chung, Y.-B., & Hinkle, D. C. (1990) *J. Mol. Biol. 216*, 927−938.
De Massy, B., Weisberg, R. A., & Studier, F. W. (1987) *J. Mol. Biol. 193*, 359−376.
Dea, I. C. M., McKinnon, A. A., & Rees, D. A. (1972) *J. Mol. Biol. 68*, 153−172.
Dunn, J. J., & Studier, F. W. (1983) *J. Mol. Biol. 166*, 477−535.
Fujisawa, H., Hamada, K., Shibata, H., & Minagawa, T. (1987) *Virology 161*, 228−233.
Fujisawa, H., Kimura, M., & Hashimoto, C. (1990) *Virology 174*, 26−34.
Houseal, T. W., Bustamante, C., Stump, R. F., & Maestre, M. F. (1989) *Biophys. J. 56*, 507−516.
Kerr, C., & Sadowski, P. D. (1972) *J. Biol. Chem. 247*, 305−310.
Lee, D. D., & Sadowski, P. D. (1983) *J. Virol. 48*, 647−653.
Lee, D. D., & Sadowski, P. D. (1985) *Can. J. Biochem. Cell Biol. 63*, 237−242.
Masker, W. E. (1982) *J. Virol. 43*, 365−367.
Masker, W. E., & Serwer, P. (1982) *J. Virol. 43*, 1138−1142.
Masker, W. E., Kuemmerle, N. B., & Allison, D. P. (1978) *J. Virol. 27*, 149−163.
Matsumoto, S., Morikawa, K., & Yanagida, M. (1981) *J. Mol. Biol. 152*, 501−516.
Minagawa, K., Matsuzawa, Y., Yoshikawa, K., Khokhlov, A. R., & Doi, M. (1994) *Biopolymers 34*, 555−558.
Minton, A. P. (1990) *Int. J. Biochem. 22*, 1063−1067.
Ogawa, H., Araki, H., & Tsujimoto, Y. (1978) *Cold Spring Harbor Symp. Quant. Biol. 43*, 1033−1041.
Panayotatos, N., & Fontaine, A. (1987) *J. Biol. Chem. 262*, 11364−11368.
Parsegian, V. A., Rand, R. P., Fuller, N. L., & Rau, D. C. (1986) *Methods Enzymol. 127*, 400−416.
Parsons, C. A., & West, S. C. (1990) *Nucleic Acids Res. 18*, 4377−4384.
Roeder, G. S., & Sadowski, P. D. (1977) *Virology 76*, 263−285.
Rosenberg, A., Lade, B. N., Chui, D.-s., Lin, S.-W., Dunn, J. J., & Studier, F. W. (1987) *Gene 56*, 125−135.
Serwer, P., Watson, R. H., & Son, M. (1990) *J. Mol. Biol. 215*, 287−299.
Serwer, P., Watson, R. H., & Hayes, S. J. (1992) *J. Mol. Biol. 226*, 311−317.
Serwer, P., Estrada, A., & Harris, R. A. (1995) *Biophys. J. 69*, 2649−2660.
Slayter, E. M., & Slayter, H. S. (1992) *Light and Electron Microscopy*, Cambridge University Press, Cambridge.
Son, M., & Serwer, P. (1992) *Virology 190*, 824−833.
Son, M., Hayes, S. J., & Serwer, P. (1988) *Virology 162*, 38−46.
Son, M., Watson, R. H., & Serwer, P. (1993) *Virology 196*, 282−289.
Steven, A. C., & Trus, B. L. (1986) in *Electron Microscopy of Proteins* (Harris, J. R., & Horne, R. W., Eds.) Vol. 5, pp 1−35, Academic Press, London.
Studier, F. W. (1969) *Virology 39*, 562−574.
Studier, F. W., & Dunn, J. J. (1983) *Cold Spring Harbor Symp. Quant. Biol. 67*, 999−1007.
Studier, F. W., Rosenberg, A. W., & Dunn, J. J. (1990) *Methods Enzymol. 185*, 60−89.
White, J. H., & Richardson, C. C. (1987a) *J. Biol. Chem. 262*, 8845−8850.
White, J. H., & Richardson, C. C. (1987b) *J. Biol. Chem. 262*, 8851−8860.
White, J. H., & Richardson, C. C. (1988) *J. Biol. Chem. 263*, 2469−2476.
Yanagida, M., Hiraoka, Y., & Katsura, I. (1983) *Cold Spring Harbor Symp. Quant. Biol. 47*, 177−187.
Zimmerman, S. B., & Minton, A. P. (1993) *Annu. Rev. Biophys. Biomol. Struct. 22*, 27−65.

BI971410B